Structural modification of the cation-ordered Ruddlesden-Popper phase $YSr_2Mn_2O_7$ by cation exchange and anion insertion.

Ronghuan Zhang, Alexandra S. Gibbs, Weiguo Zhang, P. Shiv Halasyamani and Michael A. Hayward

Supporting Information

Figure S1. Observed, calculated and difference plots from the 2-phase structural refinement of $YSrCaMn_2O_7$ against neutron powder diffraction data collected at 298 K.

Figure S2. Observed, calculated and difference plots from the structural refinement of $YSr_{0.5}Ca_{1.5}Mn_2O_7$ against neutron powder diffraction data collected at 298 K.

Figure S3. Observed, calculated and difference plots from the structural refinement of $YSr_2Mn_2O_{5.5}F_{3.5}$ against neutron powder diffraction data collected at 298 K.

Table S1. Structural parameters refined against neutron powder diffraction data collected at 300 K from $YSrCaMn_2O_7$.

Table S2. Selected bond lengths (Å) from the refined structures of $YSr_2Mn_2O_7$ [25], $YSrCaMn_2O_7$ and $YSr_2Mn_2O_{5.5}F_{3.5}$.

Table S3. Structural parameters from the refinement $YSr_{0.5}Ca_{1.5}Mn_2O_7$ against neutron powder diffraction data collected at 298 K.

Table S4. Selected bond lengths (Å) from the refined structure of $YSr_{0.5}Ca_{1.5}Mn_2O_7$.

Table S5. Fitting statistics from the structural refinement of $YSr_2Mn_2O_{5.5}F_{3.5}$ using models based on the distortions of $n = 2$ Ruddlesden-Popper phases.

Table S6. Structural parameters from the refinement $YSr_2Mn_2O_{5.5}F_{3.5}$ against neutron powder diffraction data collected at 298 K.

A description of how the octahedral rotation angles f phases were measured.

Figure S4. The torsion angles used to determine the size of the octahedral rotations in $YSr_{2-x}Ca_xMn_2O_{7-y}F_z$ phases. Parts a) and b) show the O(1)-O(5)-O(5)-O(1) torsion angle used to measure the octahedral rotation via the 'axial' oxygen-oxygen vector. Parts c) and d) show the O(4)-O(3)-O(4)-O(3) torsion angle used to measure the octahedral rotation via the 'equatorial' oxygen-oxygen vector in phases in the *P*4/*mnm* space group. Anion labels are those shown in Table S1.
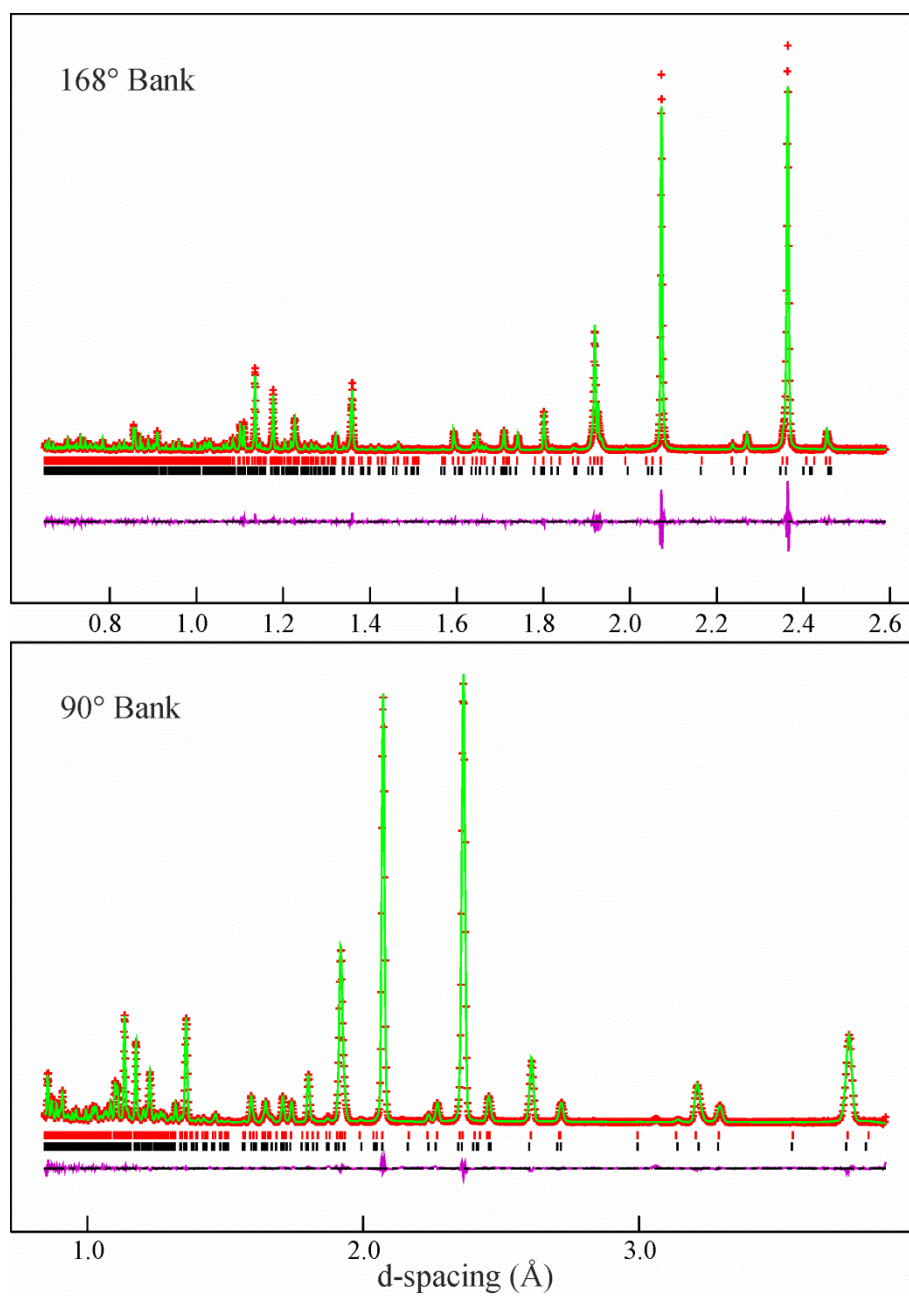
Figure S1. Observed, calculated and difference plots from the 2-phase structural refinement of YSrCaMn$_2$O$_7$ against neutron powder diffraction data collected at 298 K.

Figure S2. Observed, calculated and difference plots from the structural refinement of $YSr_{0.5}Ca_{1.5}Mn_2O_7$ against neutron powder diffraction data collected at 298 K. The excluded regions remove a contribution from the sample holder.

Figure S3. Observed, calculated and difference plots from the structural refinement of $YSr_2Mn_2O_{5.5}F_{3.5}$ against neutron powder diffraction data collected at 298 K. The excluded regions remove a peak from a binary fluoride impurity phase.
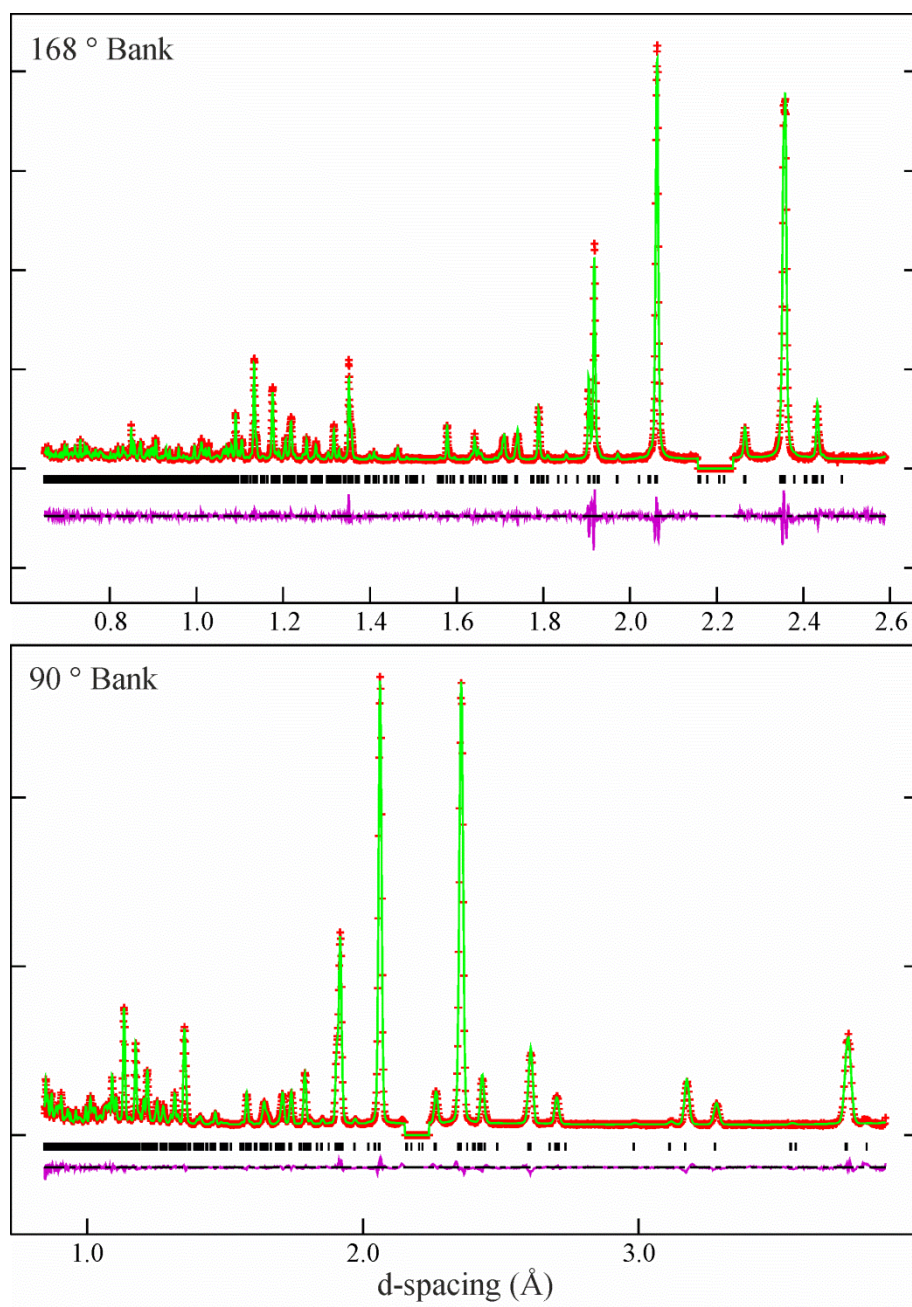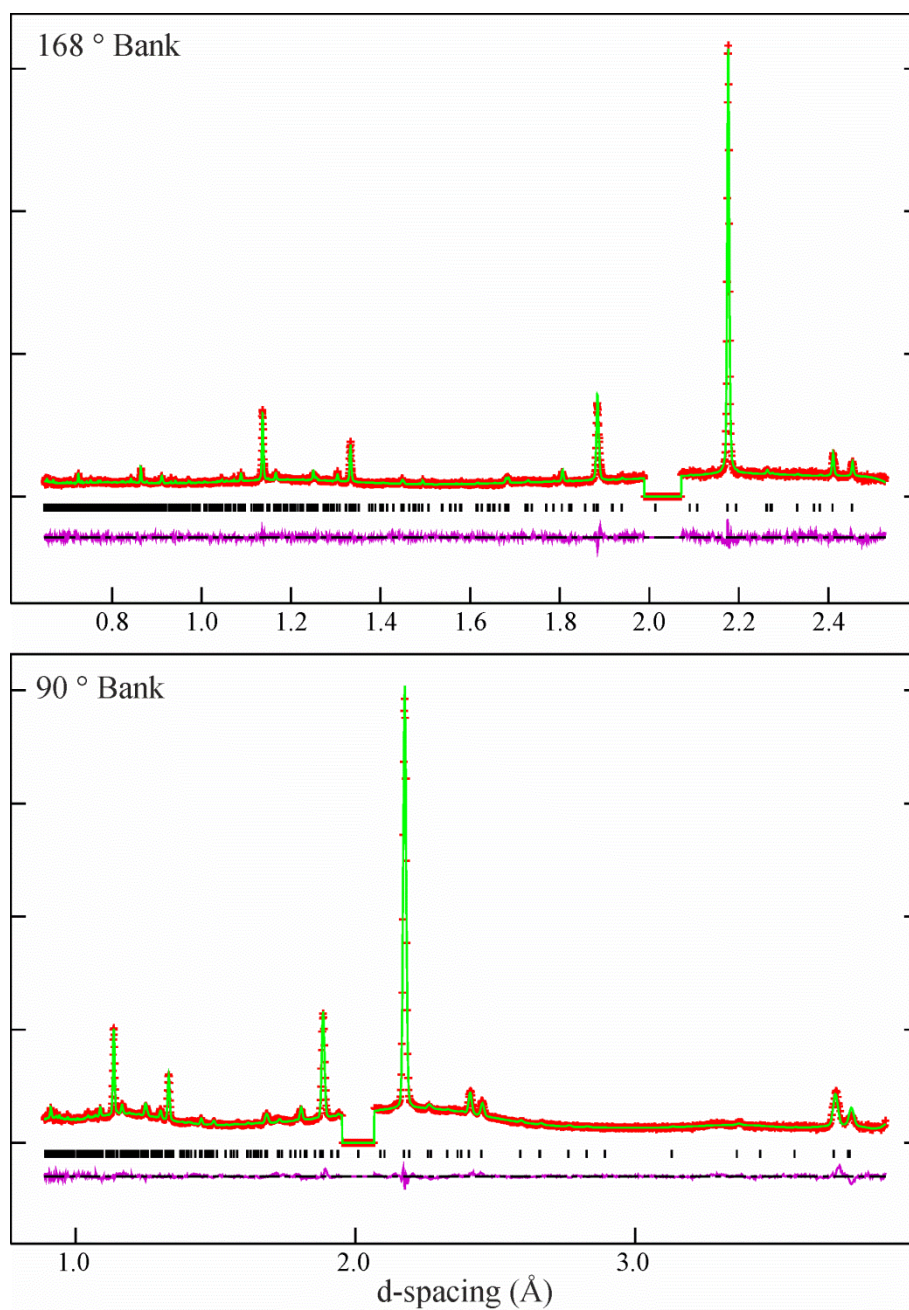
Phase 1						
Atom	site	x	y	z	Fraction	$U_{iso}(\text{Å}^2)$
Sr(1)/Ca(1)	4f	0.2517(4)	0.2517(4)	0	0.91(1)/0.09(1)	0.0062(4)
Y(1)/Sr(2)/ Ca(2)	8j	0.2632(2)	0.2632(2)	0.1831(1)	0.5/0.04(1)/ 0.46(1)	0.0039(3)
Mn(1)	8j	0.2520(5)	0.2520(5)	0.3998(1)	1	0.0012(2)
O(1)	8j	0.2126(3)	0.2126(3)	0.2987(1)	1	0.0145(3)
O(2)	8h	0	1/2	0.1024(2)	1	0.0101(3)
O(3)	4e	0	0	0.1159(1)	1	0.0082(4)
O(4)	4e	0	0	0.4083(2)	1	0.0081(4)
O(5)	4g	0.2216(3)	0.7783 (4)	0	1	0.0093(4)

YSrCaMn$_2$O$_7$ space group: *P4$_2$/mnm* (#136)
Formula weight : 438.47 g mol^{-1}, Z = 4
Phase Fraction: 65.8(1) %
a = 5.4254(1) Å b = 5.4254(1) Å c = 19.255(1) Å Volume = 566.79(1) Å^3

Phase 2						
Atom	site	x	y	z	Fraction	$U_{iso}(\text{Å}^2)$
Sr(1)/Ca(1)	4f	0.2542(8)	0.2542(8)	0	0.79(2)/0.20(2)	0.0062(4)
Y(1)/Sr(2)/ Ca(2)	8j	0.2654(5)	0.2654(5)	0.1823(2)	0.5/0.10(1)/ 0.39(1)	0.0039(3)
Mn(1)	8j	0.2568(12)	0.2568(12)	0.4018(3)	1	0.0012(2)
O(1)	8j	0.2168(8)	0.2168(8)	0.2966(2)	1	0.0145(3)
O(2)	8h	0	1/2	0.1029(3)	1	0.0101(3)
O(3)	4e	0	0	0.1168(4)	1	0.0082(4)
O(4)	4e	0	0	0.4075(4)	1	0.0081(4)
O(5)	4g	0.2216(9)	0.7783(9)	0	1	0.0093(4)

YSrCaMn$_2$O$_7$ space group: *P4$_2$/mnm* (#136)
Formula weight : 438.47 g mol^{-1}, Z = 4
Phase Fraction: 34.1 %
a = 5.4123(1) Å b = 5.4123(1) Å c = 19.325(1) Å Volume = 566.11(3) Å^3

Radiation source: Neutron Time of flight
Temperature: 298 K
χ^2 = 5.794; *wRp*= 3.91 %; *Rp* = 4.38 %.

Table S1. Structural parameters refined against neutron powder diffraction data collected at 298 K from YSrCaMn$_2$O$_7$.

Bond	YSr$_2$Mn$_2$O$_7$	YSrCaMn$_2$O$_7$		YSr$_2$Mn$_2$O$_{5.5}$F$_{3.5}$	
		Phase 1	Phase 2		
Mn-O(1)	2.032(3)	1.970(3)	2.056(9)	Mn-O/F(1)	1.872(10)
Mn-O(2) × 2	1.911(5)	1.919(3)	1.916(7)	Mn-O(2) × 2	1.884(16)
Mn-O(3)	1.912(5)	1.927(3)	1.896(7)	Mn-O(3)	1.863(17)
Mn-O(4)	1.919(5)	1.940(3)	1.969(7)	Mn-O(4)	1.932(16)
Mn-O(5)	1.961(2)	1.940(2)	1.905(8)	Mn-O(5)	1.940(9)
BVS	**3.63(4)**	**3.66(3)**	**3.62(7)**	BVS	**4.09(16)**
A(1)-O(2)× 4	2.761(6)	2.751(3)	2.760(6)	A(1)-O(2)× 4	2.660(64)
A(1)-O(3)× 2	2.879(8)	2.951(2)	2.980(7)	A(1)-O(3)× 2	2.655(95)
A(1)-O(4)× 2	2.692(6)	2.598(2)	2.595(6)	A(1)-O(4)× 2	2.931(14)
A(1)-O(5)× 2	2.639(7)	2.574(3)	2.582(7)	A(1)-O(5)× 2	2.669(15)
A(1)-O(5) ×2	2.768(7)	2.862(3)	2.842(7)	A(1)-O(5) ×2	2.658(15)
A(2)-O(1)	2.318(2)	2.259(3)	2.240(5)	A(2)-O/F(1) × 2	2.587(12)
A(2)-O(1)× 2	2.589(5)	2.467(2)	2.479(5)	A(2)-O/F(1) × 2	2.784(12)
A(2)-O(1)× 2	2.857(5)	3.011(2)	2.999(5)	A(2)-O(2) × 2	2.920(8)
A(2)-O(2)× 2	2.535(5)	2.471(3)	2.456(6)	A(2)-O(3)	2.898(12)
A(2)-O(3)	2.474(5)	2.398(2)	2.394(5)	A(2)-O(4)	2.669(11)
A(2)-O(4)	2.557(6)	2.592(2)	2.497(6)	A(2)-F(6)	2.433(16)
				A(2)-F(6)	2.452(15)
				A(2)-F(7) × 2	2.433(6)

Table S2. Selected bond lengths (Å) from the refined structures of YSr$_2$Mn$_2$O$_7$ [25], YSrCaMn$_2$O$_7$ and YSr$_2$Mn$_2$O$_{5.5}$F$_{3.5}$.

Atom	Site	x	y	z	Fraction	U (Å^2)
Sr(1)/Ca(1)	4e	0.2513(12)	0.7497(8)	0.0019(4)	0.5/0.5	0.0013(4)
Y(2)/Ca(2)	4e	0.2694(9)	0.7385(10)	0.1819(3)	0.5/0.5	0.0074(3)
Y(3)/Ca(3)	4e	0.7467(10)	0.2729(11)	0.1839(3)	0.5/0.5	0.0074(3)
Mn(1)	4e	0.2429(19)	0.2613(17)	0.0974(3)	1	0.0020(1)
Mn(2)	4e	0.7472(20)	0.7620(18)	0.1017(3)	1	0.0020(1)
O(1)	4e	0.2773(12)	0.3107(10)	0.7981(3)	1	0.0094(2)
O(2)	4e	0.2867(13)	0.2858(11)	0.2012(11)	1	0.0094(2)
O(3)	4e	0.5096(14)	0.4879(14)	0.0875(1)	1	0.0094(2)
O(4)	4e	0.0041(18)	0.9959(16)	0.1185(1)	1	0.0094(2)
O(5)	4e	0.4990(22)	0.0045(15)	0.1048(2)	1	0.0094(2)
O(6)	4e	0.0020(20)	0.5140(15)	0.0983(2)	1	0.0094(2)
O(7)	4e	0.2172(9)	0.2057(7)	0.0009(6)	1	0.0094(2)

<div align="center">

$YSr_{0.5}Ca_{1.5}Mn_2O_7$ – space group : P2$_1$/n 1 1 (#14)

Formula weight : 414.69 g mol^{-1}, Z = 4

$a = 5.4243(1)$ Å, $b = 5.4289(1)$ Å, $c = 19.0418(3)$ Å, $\alpha = 90.007(5)$

</div>

<div align="center">

Radiation source: Neutron Time of flight

Temperature: 298 K

$\chi^2 = 7.63$; $wRp = 4.74$ %; $Rp = 4.95$ %.

</div>

Table S3. Structural parameters from the refinement $YSr_{0.5}Ca_{1.5}Mn_2O_7$ against neutron powder diffraction data collected at 298 K.

Bond	Bond length (Å)	Bond	Bond length (Å)
Mn(1)-O(1)	1.951(11)	Mn(2)-O(2)	1.995(11)
Mn(1)-O(3)	1.985(13)	Mn(2)-O(3)	1.906(13)
Mn(1)-O(4)	1.911(14)	Mn(2)-O(4)	1.978(13)
Mn(1)-O(5)	1.881(17)	Mn(2)-O(5)	1.971(16)
Mn(1)-O(6)	1.930(14)	Mn(2)-O(6)	1.893(14)
Mn(1)-O(7)	1.973(15)	Mn(2)-O(7)	1.867(15)
Sr(1)/Ca(1)-O(3)	2.498(9)		
Sr(1)/Ca(1)-O(3)	2.579(9)		
Sr(1)/Ca(1)-O(4)	3.014(9)		
Sr(1)/Ca(1)-O(4)	2.918(9)		
Sr(1)/Ca(1)-O(5)	2.781(12)		
Sr(1)/Ca(1)-O(5)	2.748(12)		
Sr(1)/Ca(1)-O(6)	2.753(10)		
Sr(1)/Ca(1)-O(6)	2.615(10)		
Sr(1)/Ca(1)-O(7)	2.549(9)		
Sr(1)/Ca(1)-O(7)	2.959(9)		
Sr(1)/Ca(1)-O(7)	2.482(6)		
Sr(1)/Ca(1)-O(7)	2.888(9)		
Y(2)/Ca(2)-O(1)	2.261(11)	Y(3)/Ca(3)-O(2)	2.250(11)
Y(2)/Ca(2)-O(1)	2.498(9)	Y(3)/Ca(3)-O(2)	2.514(9)
Y(2)/Ca(2)-O(1)	2.996(9)	Y(3)/Ca(3)-O(2)	2.943(9)
Y(2)/Ca(2)-O(2)	2.487(8)	Y(3)/Ca(3)-O(1)	2.290(8)
Y(2)/Ca(2)-O(2)	2.995(8)	Y(3)/Ca(3)-O(1)	3.190(8)
Y(2)/Ca(2)-O(3)	2.602(9)	Y(3)/Ca(3)-O(3)	2.523(9)
Y(2)/Ca(2)-O(4)	2.338(10)	Y(3)/Ca(3)-O(4)	2.396(10)
Y(2)/Ca(2)-O(5)	2.405(12)	Y(3)/Ca(3)-O(5)	2.486(12)
Y(2)/Ca(2)-O(6)	2.472(10)	Y(3)/Ca(3)-O(6)	2.502(10)

Table S4. Selected bond lengths (Å) from the refined structure of $YSr_{0.5}Ca_{1.5}Mn_2O_7$.

Space Group	Glazer Tilt	χ^2	wRp (%)	Rp (%)
$P4_2/mnm$ (#136)	$a^-b^0c^0/b^0a^-c^0$	5.43	4.95	4.53
$Pnnm$ (#58)	$a^-b^-c^0/b^-a^-c^0$	7.54	5.83	5.13
$Amam$ (#63)	$a^-a^-c^0/a^-a^-c^0$	5.99	5.20	5.07
$P2_1/n11$ (#14)	$a^-b^-c^-/b^-a^-c^-$	9.47	8.31	8.18
$P2_1nm$ (#31)	$a^-b^-c^+/b^-a^-c^+$	9.53	8.45	8.23
$P2_1nm$ (#31)	$a^-b^-c^{dis}/b^-a^-c^{dis}$	9.31	8.28	8.26

Table S5. Fitting statistics from the structural refinement of $YSr_2Mn_2O_{5.5}F_{3.5}$ using models based on the distortions of $n = 2$ Ruddlesden-Popper phases.

Atom	site	x	y	z	Fraction	$U_{iso}(\text{Å}^2)$
Sr(1)	$4f$	0.2521(20)	0.2521(20)	0	1	0.0139(8)
Y(1)/Sr(2)	$8j$	0.2439(13)	0.2439(13)	0.1813(1)	0.5/0.5	0.0139(8)
Mn(1)	$8j$	0.2528(22)	0.2528(22)	0.4143(3)	1	0.010(10)
O/F(1)	$8j$	0.2252(18)	0.2252(18)	0.3321(2)	0.75/0.25	0.054(29)
O(2)	$8h$	0	1/2	0.0827(4)	1	0.012(1)
O(3)	$4e$	0	0	0.0823(6)	1	0.034(4)
O(4)	$4e$	0	0	0.4002(6)	1	0.037(5)
O(5)	$4g$	0.2466(20)	0.7533(20)	0	1	0.004(1)
F(6)	$4e$	1/2	1/2	0.2482(10)	0.998(3)	0.069(7)
F(7)	$4d$	0	1/2	1/4	0.999(2)	0.041(4)
$YSr_2Mn_2O_{5.5}F_{3.5}$ space group: $P4_2/mnm$ (#136) Formula weight : 528.50 g mol^{-1}, Z = 4 $a = 5.3266(1)$ Å $c = 22.634(1)$ Å Volume = 642.19(6) Å^3						
Radiation source: Neutron Time of flight Temperature: 298 K $\chi^2 = 5.438$; $wRp = 4.95$ %; $Rp = 4.53$ %.						

Table S6. Structural parameters from the refinement $YSr_2Mn_2O_{5.5}F_{3.5}$ against neutron powder diffraction data collected at 298 K.

Measurement of octahedral rotation angles

The displacement of the manganese cations away from the center of the MnX_6 octahedra makes Mn-O-Mn bond angles a poor parameter to measure the rotations of the MnX_6 octahedra in $YSr_{2-x}Ca_xMn_2O_{7-y}F_z$ phases. We have therefore measured the size of the octahedral rotations using only the positions of the anions, via the torsion angles.

Taking $YSrCaMn_2O_7$ as an example, this phase has an $a^-b^0c^0/ b^0a^-c^0$ rotation pattern. The size of the a^- rotation was determined as half the average of the O(1)-O(5)-O(5)-O(1) and O(4)-O(3)-O(4)-O(3) torsion angles, as shown in Figure S4. The rotation angles of other phases with $P4/mnm$ space group symmetry were determined in the same way.

The octahedral rotation angles of $YSr_{0.5}Ca_{1.5}Mn_2O_7$ which forms with an $a^-b^-c^-/b^-a^-c^-$ distortion (space group $P2_1/n\ 1\ 1$) were determined in a similar way. Specifically the a^- distortion was measured as half the average of the O(2)-O(7)-O(7)-O(1) and O(3)-O(4)-O(3)-O(4) torsion angles when measured down the appropriate axis, while the b^- distortion was measured as half the average of the O(1)-O(7)-O(7)-O(2) and O(6)-O(5)-O(6)-O(5) torsion angles when measured down the appropriate axis. The magnitude of the c^- distortion was measured as half the average of the projection of the O3-O4-O3 and O6-O5-O6 bond angles onto the xy-plane. Anion labels are listed in Table S3.
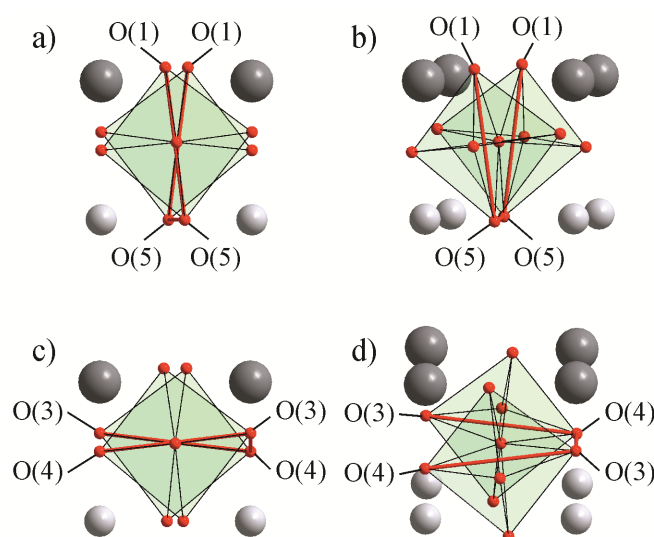
Figure S4. The torsion angles used to determine the size of the octahedral rotations in $YSr_{2-x}Ca_xMn_2O_{7-y}F_z$ phases. Parts a) and b) show the O(1)-O(5)-O(5)-O(1) torsion angle used to measure the octahedral rotation via the 'axial' oxygen-oxygen vector. Parts c) and d) show the O(4)-O(3)-O(4)-O(3) torsion angle used to measure the octahedral rotation via the 'equatorial' oxygen-oxygen vector in phases in the *P*4/*mnm* space group. Anion labels are those shown in Table S1.